Article

Not peer-reviewed version

Nano-Encapsulated *Cordyceps militaris* Grown on Germinated Black Bean Attenuates PM- and LPS-Induced Airway Inflammation

Hyo-Min Kim and Hye-Jin Park *

Posted Date: 20 April 2026

doi: 10.20944/preprints202604.1362.v1

Keywords: *Cordyceps militaris*; *Rhynchosia nulubilis*; nanoencapsulation; particulate matter; anti-inflammatory activity; PPI network and hub gene analysis

 doi:10.20944/preprints202604.1362.v1

Article

Nano-Encapsulated *Cordyceps militaris* Grown on Germinated Black Bean Attenuates PM- and LPS-Induced Airway Inflammation

Hyo-Min Kim and Hye-Jin Park *

Department of Veterinary Medicine, College of Veterinary Medicine, Konkuk University, Seoul 05029, Republic of Korea

* Correspondence: nimpi79@hanmail.net

Abstract

Exposure to particulate matter (PM) containing bacterial endotoxins triggers oxidative stress and inflammation in the respiratory epithelium. In this study, we investigated chitosan nanoparticle-encapsulated *Cordyceps militaris* grown on germinated *Rhynchosia nulubilis* (GCN) as a potential functional food–derived ingredient against PM- and lipopolysaccharide (LPS)-induced cellular damage in human lung epithelial cells. Nano-encapsulation significantly improved the antioxidant capacity and storage stability of the extract compared with the non-encapsulated form GRC. GCN markedly attenuated PM- and LPS-induced cytotoxicity and intracellular reactive oxygen species (ROS) generation in a dose-dependent manner, resulting in a therapeutic index approximately 4.5-fold higher than that of GRC. PPI network and hub gene analysis identified 120 inflammation-related genes associated with PM- and LPS-induced pulmonary responses enriched in inflammatory response, cytokine–cytokine receptor interaction, Toll-like receptor, and TNF signaling pathways. Protein-protein interaction network analysis revealed TNF, CXCL-10, IL-6, IL-1β, and CXCL-2 as key hub genes involved in these pathways. Consistent with these predictions, GCN significantly suppressed PM- and LPS-induced mRNA expression of TNF-α, CXCL-2, and TRPC6, and effectively inhibited MAPK-mediated NF-κB and AP-1 signaling pathways in A549 cells. Collectively, nano-encapsulation enhances the stability and bioactivity of *Cordyceps militaris*-based extracts and suggest that GCN may serve as a functional food-derived ingredient for protecting airway epithelial cells from oxidative stress and inflammation induced by environmental stressors.

Keywords: *Cordyceps militaris*; *Rhynchosia nulubilis*; nanoencapsulation; particulate matter; anti-inflammatory activity; PPI network and hub gene analysis

1. Introduction

The Air pollution has emerged as a major environmental concern and is widely recognized as a risk factor for respiratory dysfunction [1]. Atmospheric particulate matter (PM) is classified into coarse particles (2.5-10 μm), fine particles (< 2.5 μm), and ultrafine particles (< 100 nm), depending on particle size [2]. Among these, PM2.5 (fine PM with an aerodynamic diameter of less than 2.5 μm) can penetrate deeply into the respiratory tract and reach the alveolar region due to its small aerodynamic diameter. Exposure to PM2.5 has been shown to induce oxidative stress, excessive reactive oxygen species (ROS) generation, inflammatory responses, and apoptotic cell death in lung tissues [1,3]. PM2.5 contains various toxic constituents, including transition metals, polycyclic aromatic hydrocarbons (PAHs), volatile organic compounds (VOCs), carbonaceous particles, and endotoxins derived from gram-negative bacteria [4]. These components contribute to airway epithelial dysfunction and persistent inflammatory responses associated with environmental exposure [1].

 doi:10.20944/preprints202604.1362.v1

Importantly, interactions between PM and pathogens further exacerbate a wide range of infectious diseases. Exposure to PM can aggravate bacterial infections, as airway epithelial cell injury and immune dysregulation induced by PM enhance host susceptibility to respiratory pathogens, including *Streptococcus pneumoniae*, *Staphylococcus aureus*, *Pseudomonas aeruginosa*, *Haemophilus influenzae*, and *Moraxella catarrhalis* [1]. In addition, PM carrying lipopolysaccharide (LPS), which is abundant in organic dust and polluted air, further intensifies PM-induced lung injury by triggering cytokine release, neutrophil recruitment, and epithelial damage, even at concentrations typical of ambient environments. Consequently, inhalation of PM containing LPS is expected to provoke a stronger inflammatory response than PM alone, thereby increasing susceptibility to respiratory infections, including pneumonia [1,5]. In East Asia and South Asia, where PM2.5 levels are high, the incidence of COPD and lower respiratory tract infections is elevated [6], and the average annual number of deaths attributable to short-term PM2.5 exposure is the highest. These elevated impacts may be further exacerbated when PM carries bacterial components such as LPS, which can enhance susceptibility to lower respiratory tract infections.

Several pharmacological agents, including metformin and rosiglitazone, have been reported to attenuate PM2.5-induced inflammatory responses, while corticosteroids, antihistamines, and adrenergic receptor agonists are commonly used to manage acute respiratory symptoms. However, these approaches are generally aimed at symptomatic control and may not sufficiently address persistent oxidative stress and inflammation associated with environmental exposure. Moreover, concerns regarding long-term safety and sustained effectiveness highlight the need for complementary strategies that support respiratory health. In this context, natural products and food-derived bioactive compounds have attracted increasing interest due to their favorable safety profiles, low toxicity, and potential for long-term dietary application. Therefore, the development of functional ingredients capable of modulating oxidative stress and inflammatory responses represents a promising approach for mitigating the adverse health effects associated with PM exposure [7,8].

Cordyceps militaris (*C. militaris*) is an edible and medicinal mushroom traditionally consumed in Asia and valued for its health-promoting properties, particularly in supporting respiratory function[9,10]. It contains a variety of bioactive constituents, including cordycepin, D-mannitol, adenosine, polysaccharides, carotenoids, and ergosterol [11–15]. These compounds have been reported to exhibit antioxidant and anti-inflammatory activities, contributing to its potential role as a functional ingredient for maintaining respiratory and cardiovascular health [11–13]. However, *C. militaris* grows slowly in lepidopteran larvae and requires complicated cultivation processes. Therefore, natural fruiting bodies are scarce, making them costly to collect and difficult to produce in large quantities. This limits their use as a functional food. Therefore, artificial cultivation of *C. militaris* has emerged as a favorable alternative [16]. Germinated *Rhynchosia nulubilis (R. nulubilis)* possesses excellent nutritional characteristics, including various physiologically active compounds such as saponins, isoflavones, and anthocyanins, as well as a high protein content [17]. In particular, *R. nulubilis* exhibits anti-inflammatory effects [18], and its potent antioxidant properties may enhance immunity and help alleviate lung inflammation [19]. Therefore, we studied *C. militaris* cultured on germinated *R. nulubilis*, provided by CARI Co. Ltd., as an alternative to insect-based substrates. Extracts of *C. militaris* grown on germinated *R. nulubilis* (GRC) contain a variety of bioactive constituents, including cordycepin, adenosine, and polysaccharides from *C. militaris*, together with phenolic compounds such as isoflavones and proanthocyanidins from germinated *R. nulubilis*. These extracts exhibit multiple biological activities, including immune-enhancing, anti-allergic, anti-inflammatory, and anti-apoptotic effects [20–23]. However, the use of GRC extract is limited when administered orally due to poor membrane permeability of its hydrophilic bioactive compounds, such as cordycepin, adenosine, anthocyanins, and β-glucan [24–27], the low aqueous solubility of genistein [28], chemical instability during digestion and absorption [29,30], and poor stability during storage [31,32].

Chitosan (CHI) nanoparticles represent a promising drug delivery system for protecting bioactive compounds due to their low toxicity, biocompatibility, biodegradability, controlled release

 doi:10.20944/preprints202604.1362.v1

properties, and enhanced storage stability [30,33,34]. In our previous studies, GRC was successfully encapsulated in CHI nanoparticles (GCN), as confirmed by systematic physicochemical characterization, including zeta potential analysis, encapsulation and loading efficiencies (EE/LE), and structural assessments using X-ray diffraction (XRD) and Fourier transform infrared spectroscopy (FT-IR). The optimized formulation exhibited a nanoscale particle size of approximately 146 nm and a positive zeta potential of up to +30.68 mV, indicating favorable colloidal stability and successful incorporation of GRC. In addition, enhanced cellular uptake and improved intestinal absorption were verified, further demonstrating the functional advantages of nanoparticle encapsulation [35,36]. Based on these findings, CHI nanoparticles are expected to prevent premature degradation of encapsulated compounds by gastric acid and digestive enzymes upon oral administration and to enhance the storage stability of polyphenols, anthocyanins, and genistein, which are sensitive to temperature and light. This protection helps preserve antioxidant activity and enables the major bioactive compounds of GRC to be absorbed more effectively in the body, thereby improving biological activity and oral bioavailability [33,34,37].

Recent studies from our laboratory demonstrated that GCN exhibits enhanced cellular uptake, intestinal absorption, and protective effects against PM- or PM/LPS-induced lung inflammation in vitro and in vivo [35,36]. However, the synergistic impact of PM and bacterial endotoxins, including LPS on airway inflammatory responses and the molecular mechanisms underlying the enhanced protective effects of GCN under combined exposure conditions remain insufficiently understood. In the present study, we therefore investigated the potentiating effects of co-exposure to PM and LPS and systematically explored the molecular mechanisms by which GCN attenuates inflammatory responses. Network-based bioinformatics analysis has emerged as a useful systems-level approach for elucidating molecular mechanisms underlying complex biological responses by integrating transcriptomic data and network analysis [38,39]. Publicly available GEO transcriptomic datasets were partially utilized to identify key genes and signaling pathways associated with PM- and LPS-induced pulmonary inflammation. These findings were integrated with network-based analysis to predict potential molecular targets of GCN, followed by experimental validation in human type II alveolar epithelial cells (A549). This integrative approach enables a systematic understanding of the protective mechanisms of GCN at the molecular network level. Accordingly, this study aimed to elucidate the functional potential and underlying molecular mechanisms of GCN against PM- and LPS-induced airway inflammation by (i) identifying key genes and signaling pathways associated with inflammatory responses using a bioinformatics-based strategy, and (ii) experimentally validating its anti-inflammatory effects in A549.

2. Materials and Methods

2.1. Preparation of GRC Extract for GCN Synthesis

The hot-water extract of GRC was provided by the Cell Activation Research Institute (CARI, Seoul, Korea). 10 kilograms of GRC were extracted with 100 L of ionized water at 100 °C for 4 h, followed by filtration. The first and second extracts were combined and concentrated for use as the test sample. Furthermore, GRC was mixed with 80% methanol at a ratio of 1:20 (w/v) and extracted using a microwave oven (700 W) for 2, 4, and 6 min, respectively. The extracts were filtered through a 0.45 μm membrane filter, and the resulting supernatants were used for further analysis. GRC encapsulation with chitosan nanoparticles was performed as described in a previous study [35,36]. The GCN solution was centrifuged at 22,250 × g for 30 min (Avanti J-E; High-Speed Centrifuge; Beckman Coulter, Brea, California, USA). The centrifuged pellet was dissolved in 5 mL of a 10% sucrose solution for lyophilization.

2.2. TAC (Total Antioxidant Capacity) Assay

The TAC of the sample was determined using the phosphomolybdenum method [21]. 100 μL of sample solution (100 mg/mL) was mixed with 400 μL of the reagent solution (0.6 M sulfuric acid, 28

 doi:10.20944/preprints202604.1362.v1

mM sodium phosphate, 4 mM ammonium molybdate). The mixture was incubated at 95 °C for 90 min. After the mixture was cooled at room temperature, the absorbance of each sample was read at 695 nm using a microplate reader (Epoch, Biotek Instruments, INC., VT, USA). Ascorbic acid was used as a reference material, and ascorbic acid equivalents (AAE) were calculated using a standard curve. The total antioxidant activity of the samples was expressed as μg of AAE per mg of sample (μg AAE/mg sample).

2.3. High-Performance Liquid Chromatography (HPLC) Analysis for Adenosine

Adenosine in GRC were determined using HPLC (Agilent 1100 liquid chromatography system). A Zorbax ODS C18 column (250mm×4.6mm id, 5μm) was used. 15% methanol with 0.01M KH2PO4 was used as mobile phases with a flow rate of 1.0 mL/min. UV detection was performed at 254nm.

2.4. PM2.5 Sample Preparation

The technique for collecting and extracting PM was carried out according to a previously published protocol [23]. HEPA filters were used to collect fine particles. Briefly, filters were then placed in a 50 mL tube containing 10 mL of 75% alcohol and subjected to sonication for 30 min at 4 °C using Ultrasonic Processor Sonicator (SONICS, Newtown, Connecticut, United States of America). Subsequently, particles smaller than 2.5 μm were isolated using Whatman filter paper (1005-055, Maidstone, Kent, England). The supernatant was then concentrated under reduced pressure and preserved at −80 °C for later use.

2.5. Cell Culture and Cell Viability Assay

A549 cells were purchased from the Korean Cell Line Bank (KCLB, Seoul, Republic of Korea). Cells were maintained in RPMI 1640 (Welgene, Seoul, Republic of Korea) supplemented with 10% fetal bovine serum (Welgene) and 1% penicillin and streptomycin (Welgene). They were cultured in a 75 cm^2 cell culture flask at 37 °C in humidified 5% CO_2 incubators. According to previous study [40], cell viability was assessed using the Cell Counting Kit-8 (CCK-8) (Dojindo Laboratories, Kumamoto, Japan). The therapeutic index (TI) was calculated according to our previously established methods [41].

2.6. ROS Assay

Intracellular ROS levels were determined utilizing 2′,7′-dichlorodihydrofluorescein diacetate (DCFH-DA) as previously described [36]. This compound reacts with ROS to form the fluorescent derivative 2′,7′-dichlorodihydrofluorescein (DCF) following the supplier's guidelines (ab113851; Abcam, Cambridge, UK). The DCF-DA fluorescence was detected using Nikon Eclipse Ti Fluorescence microscopy (Point Grey Research, Richmond, BC, Canada). To assess the fluorescence intensity of DCFH-DA, a fluorescence plate reader (EnSpire, PerkinElmer, Waltham, MA, USA) was used at excitation and emission wavelengths of 485 and 535 nm, respectively [23].

2.7. Acquisition of Microarray Data and Identification of Differentially Expressed Genes (DEGs)

The Gene Expression Omnibus (GEO; http://www.ncbi.nlm.nih.gov/geo) database contains public functional genomics data, including gene expression and microarray data. In this study, the GSE193958 (3 normal lung tissues and 2 cigarette smoke- and LPS-exposed lung tissues) and GSE41684 (normal lung tissues and cigarette smoke- and LPS-exposed lung tissues) datasets were retrieved from the GPL6246 ([MoGene-1_0-st] Affymetrix Mouse Gene 1.0 ST Array) and GPL1261 ([Mouse430_2] Affymetrix Mouse Genome 430 2.0 Array) platforms. DEGs were identified, and data were normalized using GEO2R (http://www.ncbi.nlm.nih.gov/geo/geo2r), which allows users to obtain DEGs across experimental conditions by comparing two or more groups of samples based on limma R package and GEO query. For data normalization, the "force normalization" option was applied to ensure that samples displayed the same value distribution. The cutoff criteria utilized for

 doi:10.20944/preprints202604.1362.v1

screening DEGs between the case and control groups were |log (fold change; FC)| > 1 and adjusted *p*-value < 0.05 [42].

2.8. Collection of PM- and LPS-Induced Lung Inflammation-Related Genes

Target genes associated with major PM- and LPS-induced lung inflammatory conditions were acquired from GeneCards as described by Yin et al. [43]. The GeneCards database (https://www.genecards.org/) provides comprehensive information on all annotated and predicted human genes by automatically integrating large amounts of gene-centric data from 200 web sources. "Chronic obstructive pulmonary disease", "asthma", "acute respiratory distress syndrome", and "pneumonia" was chosen as a keyword to identify protein-coding genes with a GeneCards Inferred Functionality Score (GIFtS) ≥ 30 [43,44]. GIFtS leverages extensive GeneCards annotations to generate scores that estimate gene functionality. The algorithm infers functional significance from these annotations, assuming that a gene's known functionality correlates with the extent of research conducted on it.

2.9. Identification of Common and Hub Genes

We used Venny 2.1.0 (https://bioinfogp.cnb.csic.es/tools/venny/) to identify common genes between the DEGs from GSE193958 and GSE41684 as well as target genes from GeneCards, in order to identify genes associated with PM- and LPS-induced lung inflammatory responses. The common genes obtained were entered into the online database Search Tool for the Retrieval of Interacting Genes (STRING; https://string-db.org/cgi/input.pl; v12.0) to analyze significant relationships among them by constructing protein-protein interaction (PPI) networks with a confidence score threshold of 0.9, and filtering out unconnected nodes [45]. The common genes were ranked using two algorithms, Maximal Clique Centrality (MCC) and Degree, within the "CytoHubba" plug-in of Cytoscape, to identify the top 10 hub genes. Degree algorithm measures the number of edges (interactions) connected to each node. The MCC algorithm is preferred because it can detect genes within dense clusters that are likely to be biologically significant, making it particularly effective at identifying highly interconnected hub genes [46,47].

2.10. Gene Ontology (GO) and Kyoto Encyclopedia of Genes and Genomes (KEGG) Pathway Functional Analysis

Common genes were entered into the Database for Annotation, Visualization, and Integrated Discovery (DAVID; https://david.ncifcrf.gov) for GO and KEGG pathway enrichment analyses. The GO analysis included three categories: biological processes (BP), cellular components (CC), and molecular functions (MF). DAVID was used to visualize gene enrichment in the BP, CC, MF, and KEGG pathways, with a *p*-value threshold of < 0.05.

2.11. Reverse Transcriptase Polymerase Chain Reaction (RT-PCR)

Reverse transcription PCR was performed as previously described [48, 49]. Total RNA was extracted from A549 cells using TRIzol reagent (Invitrogen, Carlsbad, CA, USA). Reverse transcription was performed using a ReverTra Ace qPCR RT kit (Toyobo Biologics Inc., Osaka, Japan) according to the manufacturer's instructions. The PCR reaction was started with an initial denaturation step at 94 °C for 2 min, followed by denaturation at 94 °C for 30 s, annealing at 55 °C for 30 s, and extension at 68 °C for 1 min, followed by a cycling protocol of 35 cycles. The following primers were used: human *TNF-α* forward 5′-AAG CCT GTA GCC CAT GTT GTA G-3′, reverse 5′-GAT GGC AGA GAG GAG GTT GAC-3′; human *CXCL-2* forward 5′-CTC CTT GCC AGC TCT CCT C-3′, reverse 5′-AGC TTT CTG CCC ATT CTT GAG-3′; human *TRPC6* forward 5′-AAT TGT GCA TAC CCT CCT GC-3′, reverse 5′-TGG CAG TTT GGA TGA GCT AC-3′; and human *GAPDH* forward 5′-GAG AAG GRG GGG CTC ATT T-3′, reverse 5′-AGT GAT GGC ATG GAC TGT GG-3′ (Bionics,

 doi:10.20944/preprints202604.1362.v1

Seoul, Korea) (Bioneer, Daejeon, Korea). The levels of *TNF-α*, *CXCL-2*, and *TRPC6* mRNA were normalized to *GAPDH* mRNA levels.

2.12. Western Blot Analysis

Western blotting was performed as previously described [50]. Briefly, cells were lysed in radioimmunoprecipitation assay buffer (Cell Signaling Technology, Danvers, MA, USA) and subsequently homogenized. Proteins were isolated by centrifugation at 14,000 ×*g* for 10 min. Protein concentrations were quantified using Pierce bicinchoninic acid Protein Assay Kit (Thermo Fisher Scientific, Waltham, MA, USA). Equal amounts of protein were resolved by 10% sodium dodecyl sulfate-polyacrylamide gel electrophoresis. The separated proteins were then transferred onto nitrocellulose membranes (Bio-Rad Laboratories, Inc., Hercules, CA, USA) and blocked with 5% bovine serum albumin for 1 h at 25 °C. Overnight incubation at 4 °C was done with the membranes immersed in Tris-buffered saline with Tween (20 mM Tris, 500 mM sodium chloride, pH 7.6, 0.1% Tween 20) containing primary antibodies phosphorylated (p)-IκB (1:1000; Cell Signaling), phospho-NF-κB (1:1000; Cell Signaling), and beta-actin (1:1000; Cell Signaling) diluted as per the protocols. This was followed by a 1 h incubation with horseradish peroxidase-conjugated anti-rabbit IgG secondary antibody (1:2000; Cell Signaling). The blots were visualized using an enhanced chemiluminescence detection solution (EzWestLumi plus, ATTO Corporation, Tokyo, Japan), and images were captured and analyzed using Odyssey LCI Image software (LI-COR Biosciences, Lincoln, NE, USA). Blots are representative of at least 3 replicates.

2.13. Statistical Analysis

Data were collected from at least three experiments and are presented as mean ± standard deviation (SD). Statistical evaluation was performed using one-way analysis of variance (ANOVA) followed by Tukey honestly significant difference (HSD) test for multiple comparisons with a significant level of $\alpha = 0.05$ and 95% confidence interval ($p < 0.05$). An independent samples *t*-test was conducted to assess differences between the groups. Significance thresholds were defined as follows: $p < 0.05$, $p < 0.01$, and $p < 0.001$. Data analysis was performed using SPSS version 12 software (IBM, Chicago, IL, USA).

3. Results

3.1. Formation of Chitosan Nanoparticles from Different GRC Extracts and Their Antioxidant Potential and Bioactive Compounds

During the chitosan nanoparticle preparation, precipitate formed with the 80% methanol GRC extract, indicating unsuccessful nanoparticle formation (Figure 1A). No precipitate formed with the hot-water GRC extract, and centrifugation after TPP addition yielded a nanoparticle pellet, which was used for subsequent preparation (Figure 1B). To compare the antioxidant activity and storage stability of GRC and GCN, three different samples-GRC stored at 4 °C, GRC stored at room temperature, and GCN stored at room temperature-were analyzed using a TAC assay. The results demonstrated that GCN exhibited higher antioxidant capacity than GRC and showed improved stability after 20 days of storage at room temperature (Figure 1C). In addition, the adenosine content in GRC was 0.36 ± 0.00 mg/g (Table 1).

Table 1. Adenosine content in GRC determined by HPLC.

Compounds	Concentrations of analytes in 40mg/mL GRC (μg/mL) [a]	Contents (mg/g-GRC) [b]
Adenosine	14.19±0.07	0.36±0.00

The mean values of three independent determinations are presented. [a] Values (μg/mL) indicate the concentration of analytes in a 50% methanol extract of GRC prepared at 40 mg/mL. [b] Contents (mg/g) in GRC on a dry weight basis.

 doi:10.20944/preprints202604.1362.v1

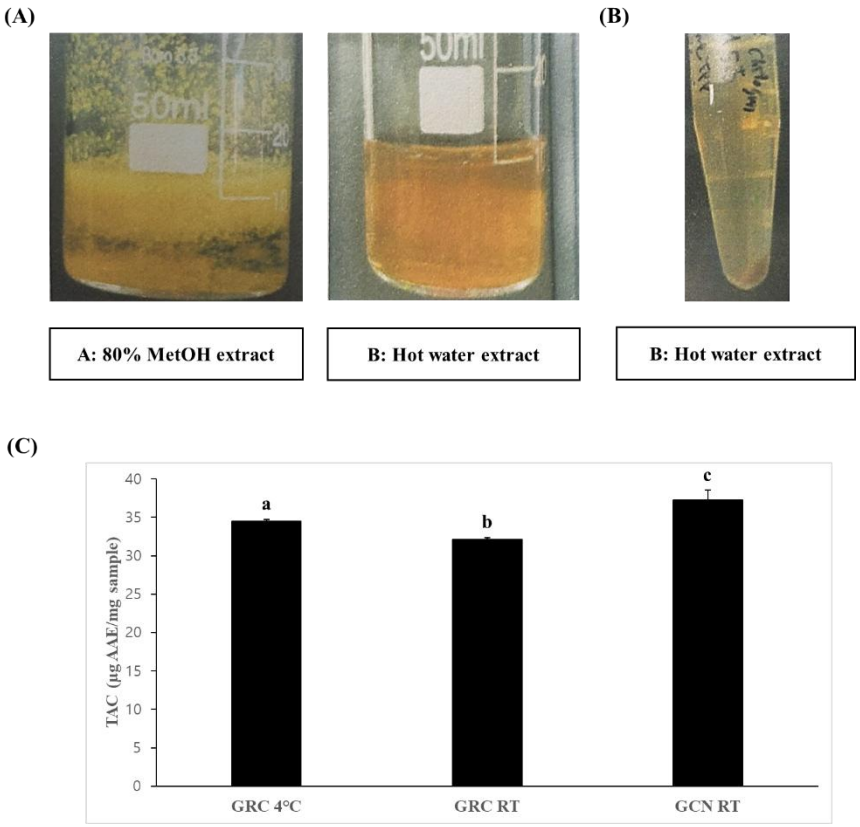

Figure 1. Preparation of GRC-encapsulated chitosan nanoparticles and their antioxidant activity and storage stability. (A) Precipitate formation observed in the 80% methanolic GRC extract after the addition of chitosan. (B) Nanoparticles separated by centrifugation at 14,240 × g. (C) Total antioxidant capacity (TAC) of GRC stored at 4 °C and at room temperature, and GCN stored at room temperature for 20 days. TAC was expressed as μg of ascorbic acid equivalents (AAE) per mg of sample. The experiments were repeated three times and results are presented as mean ± standard deviation (SD). Statistically significant comparisons between groups were analyzed using one-way ANOVA with Tukey's honestly significant difference (HSD) post-test. a-c, Bars with different letters differ significantly at $p < 0.05$ by Tukey HSD test.

3.2. GCN Suppresses PM- and LPS-Induced A549 Cell Death and In Vivo Toxicological Evaluation

Co-treatment with PM and LPS significantly reduced A549 cell viability in a dose-dependent manner compared with the PM-treated groups (50, 100, and 200 μg/mL) and the untreated control ($p < 0.05$) (Figure 2A). GCN significantly decreased PM and LPS co-treated A549 cell death, showing greater suppressive effect compared to GRC at 200 μg/mL ($p < 0.05$) (Figure 2B). The median effective dose (ED50) indicates the concentration of GCN or GRC required to elicit a half-maximal protective effect against PM- and LPS-induced A549 cell death. By contrast, The half-maximal inhibitory concentration (IC50) indicates the concentration at which GCN or GRC alone reduces cell viability by 50%. The ED50 of GRC in A549 cells was 218.19 ± 55.19 μg/mL, whereas the ED50 of GCN was 145.45 ± 19.18 μg/mL, representing a reduction of approximately 1.5-fold for GCN. In addition, the IC50 of GRC was 735.75 ± 136.53 μg/mL, whereas the IC50 of GCN was 2327.90 ± 568.15 μg/mL, approximately 3-fold higher than GRC (Figure 2C). The TI was calculated to compare the relative safety of GCN and GRC regarding overdose risk, yielding a TI of 15.85 ± 1.67 for GCN and 3.49 ± 0.97 for GRC. This represents an approximately 4.5-fold increase in TI for GCN compared to that for GRC, indicating a statistically significant enhancement in the safety and efficacy of GCN in inhibiting PM- and LPS-induced A549 cell death (independent samples *t*-test, $p < 0.001$).

 doi:10.20944/preprints202604.1362.v1

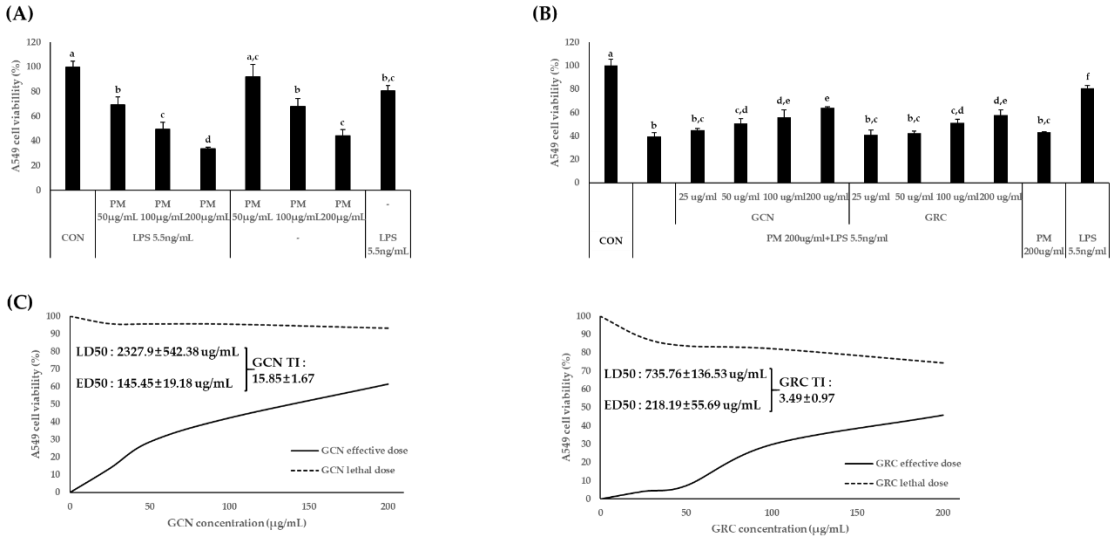

Figure 2. Effects of GRC, GCN, PM, and LPS on the viability of type II alveolar epithelial cells (A549). (A) The viability of cultured A549 cells treated with various concentrations (50, 100, and 200 μg/mL) of PM and LPS (5.5 ng/mL) for 24 h. LPS was used as a positive control. (B) Effects of GCN and GRC on the viability of cultured A549 cells exposed to PM (200 μg/mL) and LPS (5.5 ng/mL). A549 cells were treated with various concentrations (25, 50, 100, and 200 μg/mL) of GCN and GRC for 24 h. PM and LPS were used as a positive control. A549 cell viability was assessed using Cell Counting Kit-8 (CCK-8) assays. (C) Dose-response curve of GCN and GRC on A549 cell viability. Data are expressed as the mean value ± SD. a-f, Bars with different letters differ significantly at $p < 0.05$ by Tukey HSD test. Data comparisons between two groups were analyzed using the independent samples *t*-test ($p < 0.01$).

3.3. GCN Reduces PM- and LPS-Induced ROS Production in A549 Cells

To establish a robust oxidative stress model, intracellular ROS production was first evaluated in A549 cells exposed to PM and LPS. Combined PM and LPS stimulation markedly increased intracellular ROS levels by 11.60 ± 0.54-fold compared with the control group and by 2.31 ± 0.16-fold compared with PM-treated cells alone ($p < 0.05$), demonstrating a synergistic effect of PM and LPS on oxidative stress induction (Figure 3A, B). Based on this validated oxidative stress condition, we next investigated the intracellular ROS scavenging activity of GCN. GCN treatment significantly suppressed PM- and LPS-induced intracellular ROS production, reducing ROS levels to 0.20 ± 0.05-fold relative to the stimulated group ($p < 0.05$), as indicated by decreased fluorescence intensity. Furthermore, GCN exhibited significantly greater antioxidant activity than GRC, with intracellular ROS levels in GCN-treated cells being 0.59 ± 0.00-fold lower than those observed in GRC-treated cells ($p < 0.05$; Figure 3C, D). Collectively, these results demonstrate that combined PM and LPS exposure effectively induces intracellular oxidative stress, and that GCN potently attenuates ROS overproduction under these oxidative stress conditions, supporting its antioxidant efficacy.

 doi:10.20944/preprints202604.1362.v1

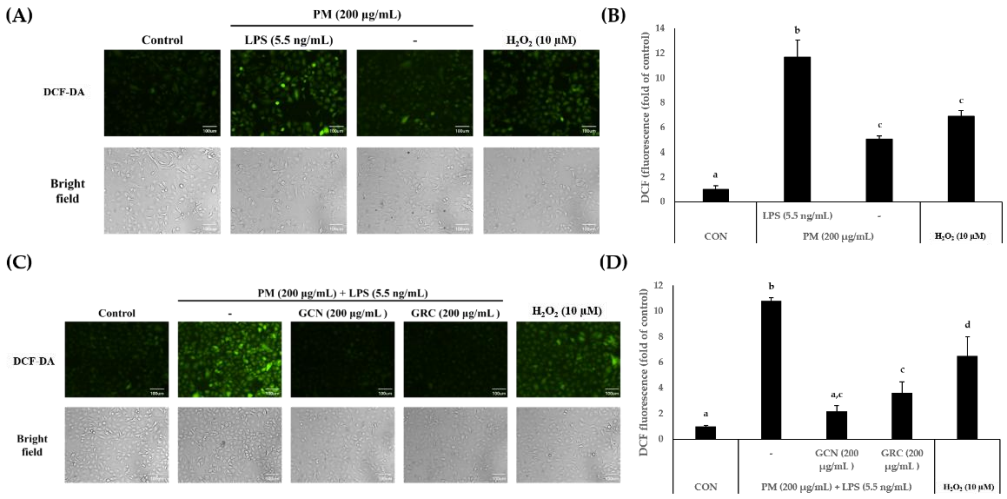

Figure 3. Scavenging effects of GCN on PM- and LPS-induced intracellular reactive oxygen species (ROS) in A549 cells. (A, C) Intracellular ROS were detected using fluorescence microscopy (Nikon Eclipse Ti microscope, Point Grey Research, Richmond, BC, Canada) after 2′,7′-dichlorodihydrofluorescein diacetate (DCF-DA) staining. Hydrogen peroxide (H_2O_2), an ROS inducer, was used as a negative control. (B, D) ROS scavenging effect of 200 μg/mL of GCN and 200 μg/mL of GRC on PM- and LPS-induced intracellular ROS in A549 cells. The intercellular level of ROS was measured using DCF-DA at a wavelength of 485/535 (Ex/Em). Data are expressed as the mean value ± SD. a-d, Bars with different letters differ significantly at $p < 0.05$ by Tukey HSD test [35].

3.4. DEG Analysis Using GEO2R and DAVID for Biomarker Identification

We explored gene expression datasets to identify DEGs between PM- and LPS-treated and normal samples. Given the similarities in the chemical compositions of cigarette smoke and PM [51,52], the GSE193958 (n = 5) and GSE41684 (n = 8) datasets, which included cigarette smoke- and LPS-treated samples, were examined, yielding 1,300 (935 upregulated and 365 downregulated) and 651 DEGs (432 upregulated and 219 downregulated), respectively ($|logFC| > 1$, adjusted $p < 0.05$) [42]. Additionally, COPD-related target genes were retrieved from GeneCards (7,808 protein-coding genes, GIFtS ≥ 30) [43,44] and overlapped with these DEGs using A Venn diagram, identifying 120 common genes associated with major PM- and LPS- induced lung inflammatory conditions (Figure 4A). COPD was selected as a representative inflammation-related condition triggered by PM and LPS [53–55], including asthma, acute respiratory distress syndrome (ARDS), and pneumonia, because it showed significant overlap with the DEGs identified in the GSE193958 and GSE41684 datasets (data not shown).To explore the key functional and biological characteristics of the 120 common genes, GO and KEGG pathway analyses were performed using the DAVID database. The GO ontology consists of three categories: BP, MF, and CC. The top five enriched terms in each category are shown in Figure 4B. In the BP analysis, common genes were significantly associated with inflammatory response (GO:0006954), cellular response to LPS (GO:0071222), immune response (GO:0006955), chemokine-mediated signaling pathway (GO:0070098), and positive regulation of tumor necrosis factor (TNF) production (GO:0032760). In MF analysis, genes were primarily enriched for chemokine activity (GO:0008009), protein binding (GO:0005515), cytokine activity (GO:0005125), identical protein binding (GO:0042802), and C-X-C motif chemokine receptor (CXCR) binding (GO:0045236). For the CC analysis, the genes were mainly involved in the extracellular space (GO:0005615), extracellular region (GO:0005576), external side of the plasma membrane (GO:0009897), cell surface (GO:0009986), and extracellular matrix (GO:0031012). KEGG pathway analysis revealed that the common genes were mainly associated with the cytokine-cytokine receptor interaction (mmu04060), toll-like receptor signaling pathway (mmu04620), TNF signaling pathway (mmu04668), IL-17 signaling pathway (mmu04657), and viral protein interaction with cytokine and cytokine receptor (mmu04061) (Figure 4C).

 doi:10.20944/preprints202604.1362.v1

To investigate the PPIs among the 120 common genes, they were uploaded to the STRING database with the maximum number of interactors set to 0 and the minimum required interaction score set to the highest confidence level (≥ 0.9) [45]. This analysis generated a PPI network comprising 118 nodes and 1,178 edges (Figure 4D). Next, Cytoscape plug-in CytoHubba was used to identify key hub genes within the network. The top 10 hub genes were identified by applying both the MCC and Degree algorithms to the PPI network, and the 8 overlapping genes were *TNF*, *CXCL-10*, *CXCL-1*, *IL-6*, *IL-1β*, *CCR2*, *CXCL-2*, and *CCL4*. These genes are likely to play critical roles in COPD induced by PM and LPS exposure (Figure 4E). Among them, *TNF*, *CXCL-10*, *IL-6*, *IL-1β*, and *CXCL-2* were also ranked among the top genes in the GEO2R differential expression analysis and are involved in the TNF signaling pathway (mmu04668).

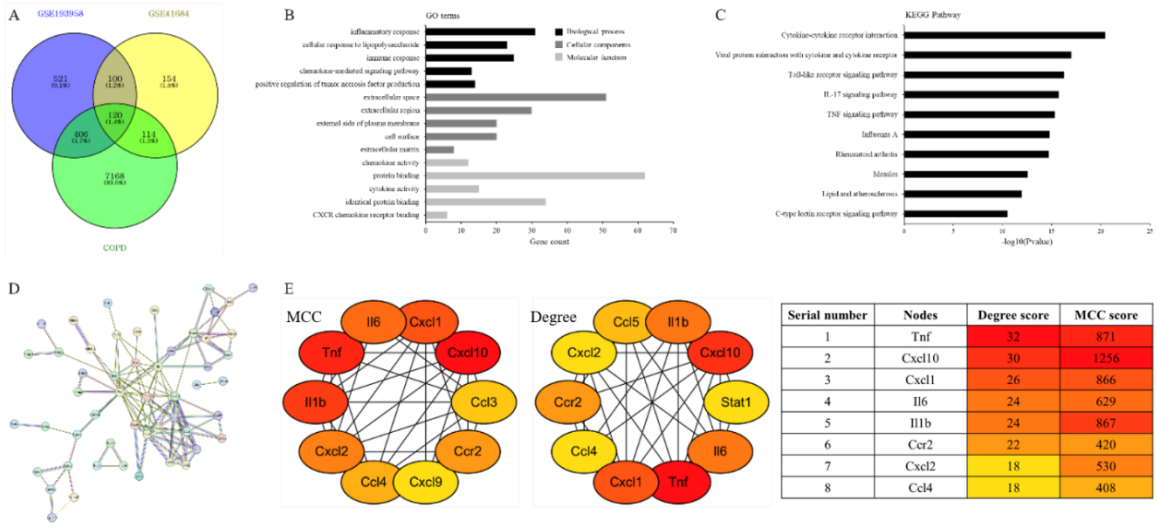

Serial number	Nodes	Degree score	MCC score
1	Tnf	32	871
2	Cxcl10	30	1256
3	Cxcl1	26	866
4	Il6	24	629
5	Il1b	24	867
6	Ccr2	22	420
7	Cxcl2	18	530
8	Ccl4	18	408

Figure 4. Functional enrichment analysis of common genes, followed by hub gene screening in the protein-protein interaction (PPI) network using CytoHubba plug-in. (A) Venn diagram showing the common genes between differentially expressed genes (DEGs) from GSE193958 and GSE41684 and chronic obstructive pulmonary disease (COPD)-related target genes. (B) Enrichment of biological process (BP), cellular components (CC), and molecular function (MF) of the common genes. (C) Kyoto Encyclopedia of Genes and Genomes (KEGG) pathway enrichment analysis of the common genes. (D) PPI network of the common genes was constructed using the STRING online database. Edges represent interactions between common genes. (E) Top 10 hub genes were ranked by CytoHubba using the following methods: Degree and Maximal clique centrality (MCC) scores.

3.5. GCN Attenuates Cytokine and Chemokine Expression in PM- and LPS-Treated A549 Cells

To evaluate the anti-inflammatory potential of GCN under inflammatory conditions, A549 cells were stimulated with PM and LPS. GCN significantly reduced the PM- and LPS-induced mRNA expression of the neutrophil chemoattractant *CXCL-2* by 87.9% ± 1.26 compared with the stimulated group ($p < 0.05$), demonstrating a strong inhibitory effect on chemokine induction. In addition, GCN pretreatment significantly attenuated the mRNA expression of *TNF-α*, in PM- and LPS-stimulated A549 cells ($p < 0.05$). Notably, *TNF-α* mRNA levels were reduced to 0.13 ± 0.00-fold relative to the PM- and LPS-treated group, indicating potent suppression of cytokine signaling by GCN (Figure 5). Given the established role of TRPC6 in CXCL-2-mediated neutrophil migration and chemotaxis, we further examined TRPC6 expression. Consistent with the suppression of CXCL-2, GCN significantly attenuated the PM- and LPS-induced upregulation of *TRPC6* mRNA, supporting a coordinated inhibitory effect of GCN on the CXCL-2/TRPC6 inflammatory axis ($p < 0.05$).

 doi:10.20944/preprints202604.1362.v1

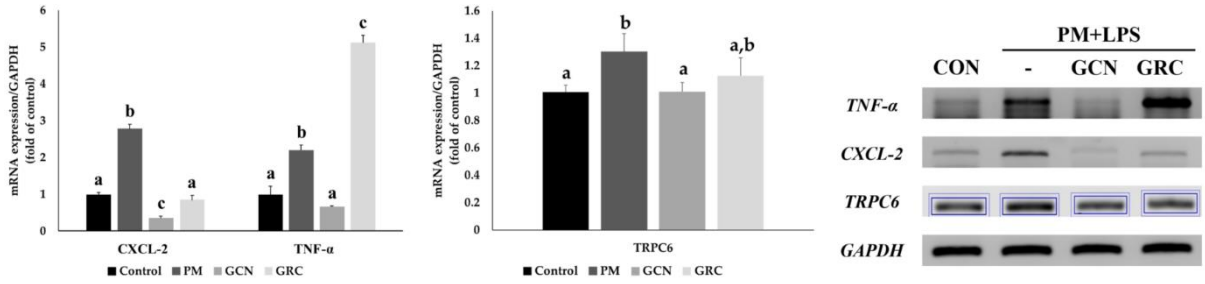

Figure 5. Effects of GCN on the levels of *CXCL-2, TNF-α, and TRPC6* mRNA expression in PM and LPS-stimulated A549 cells. A549 cells were pretreated with GCN (200 μg/mL) and GRC (100 μg/mL) for 1 h, followed by treatment with 200 μg/mL PM and 5.5 ng/mL LPS for 12 h. The levels of *CXCL-2, TNF-α, and TRPC6* mRNA was determined using quantitative reverse transcription-polymerase chain reaction. Bar heights indicate the percentages of *CXCL-2, TNF-α, and TRPC6* mRNA at the indicated concentrations of samples, relative to the values determined in PM and LPS-treated A549 cells. Data are expressed as the mean value ± SD. a-c, Bars with different letters differ significantly at $p < 0.05$ by Tukey HSD test [23,40].

3.6. GCN Inhibits PM- and LPS-Induced Activation of MAPK-Mediated NF-κB/Activator Protein 1 (AP-1) Signaling Pathways

Based on KEGG pathway analysis identifying the Toll-like receptor and TNF signaling pathway as key regulators of the NF-κB, MAPK, and AP-1 signaling cascades, this study was conducted to elucidate the molecular mechanisms underlying the anti-inflammatory activity of GCN. GCN significantly attenuated the PM- and LPS-induced phosphorylation of extracellular signal-regulated kinase (ERK), c-Jun N-terminal kinase (JNK), and p38 mitogen-activated protein kinase (p38 MAPK), as well as activation of the NF-κB signaling cascade, including phosphorylated inhibitor of κB (p-IκB), phosphorylated NF-κB (p-NF-κB), and the AP-1 signaling cascade, including phosphorylated c-Jun (p-cJun) in A549 cells ($p < 0.05$; Figure 6). Although both GCN and GRC (200 μg/mL) effectively reduced PM- and LPS-induced inflammatory signaling, GCN exerted significantly greater inhibitory effects than GRC on the activation of the MAPK (ERK, JNK, and p38 MAPK) and NF-κB signaling pathways, demonstrating its superior anti-inflammatory efficacy under inflammatory conditions ($p < 0.05$). These results indicate that GCN robustly suppresses PM- and LPS-induced inflammatory responses by coordinately inhibiting MAPK and NF-κB signaling pathways, highlighting its potential as a functional food-derived anti-inflammatory agent.

 doi:10.20944/preprints202604.1362.v1

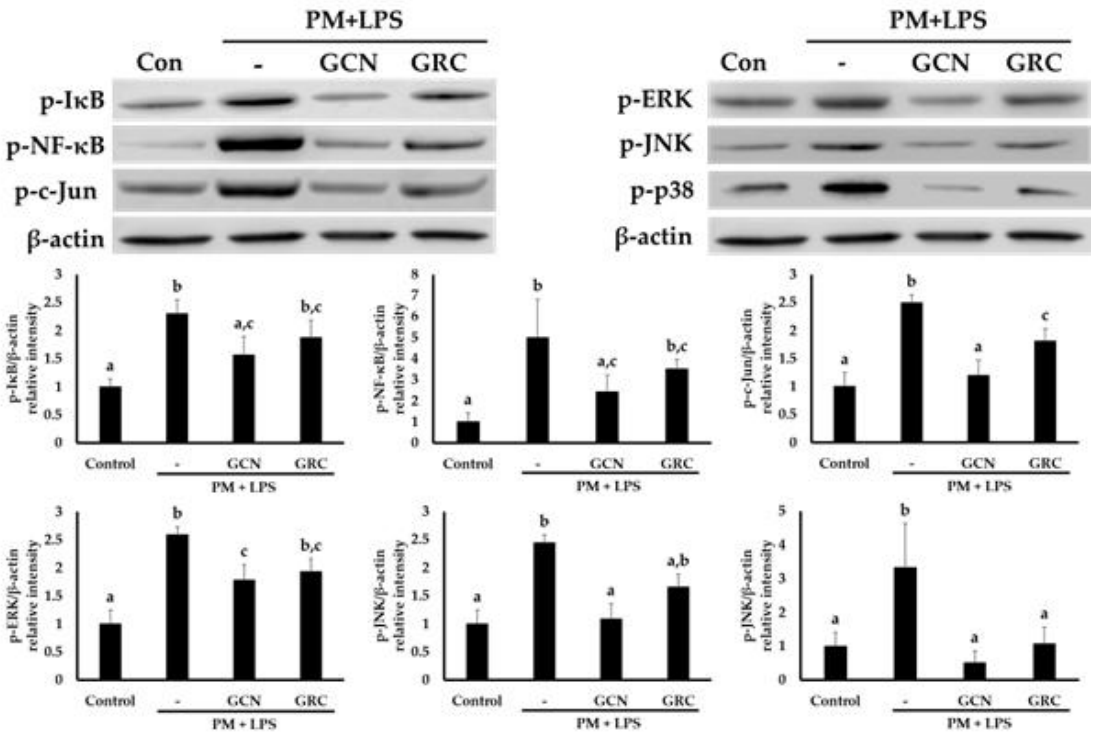

Figure 6. GCN inhibits PM- and LPS-induced inflammatory responses in A549 cells by suppressing the activation of NF-κB, AP-1, and MAPK pathways. A549 cells were pretreated with 200 μg/mL GCN or 200 μg/mL GRC for 1 h, followed by treatment with 200 μg/mL of PM and 5.5 ng/mL of LPS for 1 h. Whole-cell lysates were processed for western blotting analysis and probed with the indicated antibodies. p-IκB, p-NF-κB, p-c-Jun, p-ERK, p-JNK protein expression levels in A549 cells were detected using western blotting. Relative intensity is shown as the means ± SD of three independent experiments. a-c, Bars with different letters differ significantly at $p < 0.05$ by Tukey HSD test.

4. Discussion

Previous studies have demonstrated that GRC exhibits immune-enhancing, anti-allergic, anti-inflammatory, anti-apoptotic, and antioxidant effects [20,21,35,36]. These beneficial effects are attributed to the diverse bioactive compounds present in GRC. Specifically, GRC contains antioxidants, such as cordycepin, adenosine, polysaccharides, D-mannitol, carotenoids, ergosterol, and bioactive proteins derived from *C. militaris*, as well as novel isoflavones, including genistein 4-O-β-D-glucoside 4″-O-methylate (CGNMII), daidzein 7-O-β-D-glucoside 4″-O-methylate (CDGM), genistein 7-O-β-D-glucoside 4″-O-methylate (CGNMI), and glycitein 7-O-β-D-glucoside 4″-O-methylate (CGLM), proteins, proanthocyanidins, and polyphenols derived from *R. nulubilis*. These bioactive compounds, derived from *C. militaris*, attenuate inflammatory responses and ROS production while enhancing antioxidant enzyme activity under PM exposure conditions, thereby reducing oxidative stress [13,15,21,23,56–58].

However, its biological effectiveness following oral intake may be limited by inadequate physicochemical stability and bioavailability, as key constituents such as phenolic compounds and cordycepin are susceptible to rapid metabolism and limited absorption in the gastrointestinal tract [59–61]. To address these limitations, we formulated GRC into a CHI-based nanoparticle to improve stability, protect labile bioactives from degradation, and enhance cellular uptake [35,36]. Consistent with the reported protective role of CHI nanoencapsulation against gastrointestinal and storage-related degradation [35,62], both the hot-water extract of GRC and GCN exhibited substantial TAC in the present study, indicating that intrinsic GRC constituents substantially contribute to antioxidant potential. Notably, however, GCN retained significantly higher TAC than GRC after 20 days of

 doi:10.20944/preprints202604.1362.v1

storage, supporting the notion that chitosan-based encapsulation effectively stabilizes labile antioxidant components and preserves functional activity over time.

The antioxidant capacity of GRC likely reflects the presence of water-soluble bioactives such as cordycepin [20,21,63], adenosine [63], polysaccharides [20,21], phenolic compounds [22,23,40,63], isoflavones, and anthocyanins, as previously characterized in our studies.

Importantly, the improved TAC retention observed for GCN suggests that nanoencapsulation protects these constituents from chemical and enzymatic degradation, which may contribute to the superior functional performance observed in subsequent cellular experiments. Given that excessive intracellular ROS generation is a critical upstream event in PM- and LPS-induced lung inflammation, the ability of GCN to modulate oxidative stress at the cellular level was subsequently evaluated using ROS-sensitive assays, which are discussed in detail in the following sections.

PM2.5 contains organic components (e.g., PAHs, VOCs) and inorganic substances (e.g., sulfates, nitrates, and transition metals) that together promote ROS generation [64–66]. PAHs activate the aryl hydrocarbon receptor (AhR), inducing cytochrome P450 1A1 (CYP1A1), which generates superoxide and electrophilic quinones during PAH metabolism [67–72]. Quinones undergo redox reactions, leading to the generation of superoxide anion ($O_2^{\bullet-}$) and hydroperoxyl radicals (HOO•) [70–72]. Water-soluble ions such as sulfate (SO_4^{2-}) and nitrate (NO_3^-) present in PM2.5 indirectly enhance ROS production by promoting Fenton reactions. After inhaled PM reaches the alveoli, SO_4^{2-} and NO_3^- dissolve easily in the wet alveolar wall [73]. Particularly, SO_4^{2-} binds to Fe^{2+}, stabilizing it and enhancing the Fenton reaction, thereby increasing HO· production and inducing damage to alveolar cells [73–75].Transition and heavy metals (e.g., Fe, Cu, Mn, Pb, As, Cd) further amplify oxidative stress and deplete antioxidant defenses [76–82]. Additionally, LPS in PM activates Toll-like receptor (TLR) 4 signaling, upregulating NADPH oxidase 2 (NOX2) and NADPH oxidase 4 (NOX4), further increasing ROS generation in alveolar epithelial cells [83,84]. Accordingly, we observed that co-exposure to PM and LPS induced higher intracellular ROS levels in A549 cells than PM exposure alone, consistent with reports describing synergistic oxidative stress under combined exposure [85–87].

Notably, GCN markedly reduced PM- and LPS-induced intracellular ROS levels compared with GRC, indicating that nanoencapsulation enhances the antioxidant efficacy of GRC in vitro. This enhanced activity may stem from improved cellular delivery and protection of labile compounds during uptake, thereby increasing the effective intracellular availability of antioxidant constituents [27,59,88]. Mechanistically, several GRC-derived constituents-such as cordycepin, adenosine, polysaccharides, D-mannitol, ergosterol, and bioactive proteins from *C. militaris*, and proanthocyanidins, and polyphenols from *R. nulubilis* as well as novel isoflavones (CGNMII, CDGM, CGNMI, and CGLM) from GRC-may contribute to ROS mitigation, enhancement of antioxidant enzyme activity, and suppression of inflammation [13,15,21,23,56,57]. Cordycepin and adenosine, the main bioactive nucleosides present in *C. militaris* [89], increase cellular antioxidant defenses by upregulating superoxide dismutase (SOD), glutathione peroxidase, and catalase (CAT), while diminishing $O_2^{\bullet-}$ and hydrogen peroxide (H_2O_2) production, thereby protecting cells from oxidative damage [90,91]. Consistent with these reports, HPLC analysis confirmed the presence of adenosine in GRC, which may contribute to the observed antioxidant activity by enhancing cellular antioxidant defenses. Polyphenols present in *C. militaris* and *R. nulubilis (*such as anthocyanins*)* have potent antioxidant properties that increase the expression of antioxidant enzymes such as SOD and GSTs [92] and scavenge singlet oxygen and various ROS through their hydroxyl groups, thereby reducing lipid peroxidation and oxidative damage [92,93]. Furthermore, polysaccharides from *C. militaris* enhance antioxidant defenses by increasing the activities of antioxidant enzymes, such as SOD and CAT [94]. β-glucan, one of the major bioactive compounds in *C. militaris*, exhibits notable antioxidant activity by scavenging HO· and chelating metal ions. These effects are likely attributed to its functional groups (–OH, C=O, and C–H) which may contribute to mitigating oxidative damage [95–97]. Collectively, these effects provide plausible biochemical support for the ROS-suppressive phenotype observed with GCN.

 doi:10.20944/preprints202604.1362.v1

The reduction in intracellular ROS levels was accompanied by improved cell viability in PM- and LPS-exposed A549 cells, supporting a protective role against co-exposure-induced cytotoxicity. This finding is biologically meaningful because alveolar type II (AT2) cells play a crucial role in maintaining alveolar homeostasis, regulating surfactant production, and supporting epithelial regeneration. Excessive damage to AT2 cells may impair tissue repair processes and disrupt airway epithelial integrity. PM and LPS exposure have been reported to induce apoptotic cell death and functional impairment in AT2 cells, thereby aggravating oxidative stress and inflammatory responses in the lung [98–104]. Consistent with these reports, we observed a significant viability decline following PM and LPS co-treatment. Importantly, the higher TI of GCN compared with GRC indicates greater protective activity at lower cytotoxic concentrations, which aligns with improved uptake and bioavailability commonly associated with chitosan-based nanoparticles [35,41,62,105,106]. These results suggest that GCN may represent a superior functional formulation for mitigating particle-associated epithelial injury. CHI nanoparticles possess a positively charged surface that can promote electrostatic interactions with negatively charged cellular membranes and mucosal surfaces, thereby enhancing mucoadhesion, prolonging residence time at absorption sites, and facilitating sustained release of encapsulated compounds [35,41,105,106]. In line with these concepts, our previous work showed that nanoformulation improved the intestinal absorption efficiency of GRC by increasing solubility, and enhancing permeability of water-soluble constituents, which could contribute to greater systemic exposure and sustained functional activity [35,62].

PM- and LPS-induced ROS are well recognized as key mediators of airway inflammatory responses, contributing to mucus hypersecretion, epithelial dysfunction, and impaired mucociliary clearance. Although oxidative stress and chronic inflammation are known to play critical roles in respiratory dysfunction associated with environmental exposure, the molecular mechanisms underlying PM- and LPS-triggered inflammatory signaling remain incompletely defined. To further elucidate the inflammatory pathways associated with PM- and LPS-induced epithelial injury, transcriptomic analyses from two relevant datasets (GSE193958 and GSE41684) from cigarette smoke– and LPS-exposed lung tissues were integrated with inflammation-related gene profiles to identify key signaling pathways and regulatory factors involved in exposure-associated pulmonary inflammation. Given that PM and cigarette smoke share chemically complex constituents and overlapping toxicological properties, the identified pathways may provide broader insight into environmentally induced airway inflammatory responses [51,107,108]. Network analysis identified 120 genes enriched in cytokine–cytokine receptor interaction, Toll-like receptor (TLR) signaling, IL-17 signaling, and TNF signaling. These pathways converge on central inflammatory regulators, including the TLR4/MyD88 axis and downstream MAPK, NF-κB, and AP-1 cascades, which are known to mediate pro-inflammatory cytokine production under oxidative and inflammatory stress conditions [109–115]. Using CytoHubba, hub genes including TNF, CXCL-10, IL-6, IL-1β, and CXCL-2, which were consistently highly ranked and upregulated across datasets, were identified, suggesting key roles in inflammatory amplification and immune cell recruitment during exposure-associated airway inflammation [116–119]. The relevance of these hub genes and major inflammatory signaling molecules was experimentally validated in PM- and LPS-treated A549 cells using RT-PCR and Western blot analysis.

Notably, GCN significantly suppressed the expression of key cytokines, chemokines, and hub regulators, supporting a mechanistic link between nanoformulation-mediated ROS attenuation and downstream modulation of inflammatory signaling networks.At the signaling level, PM-induced oxidative stress and TLR4 activation can trigger MAPK (p38/JNK/ERK) and transcription factor cascades (NF-κB and AP-1), culminating in excessive cytokine/chemokine production, including TNF-α, IL-1β, IL-6, and CXCL-2 [66,84,120–122]. Our results showed that GCN inhibited the expression of TNF-α, CXCL-2, and TRPC-6 and reduced the phosphorylation of MAPK, NF-κB, and c-Jun in PM- and LPS-exposed lung epithelial cells, indicating suppression of MAPK–NF-κB/AP-1 signaling.

 doi:10.20944/preprints202604.1362.v1

CXCL-2 binds to CXCR2, promoting neutrophil migration and activation, angiogenesis, and alveolar epithelial cell proliferation. Inflammatory stimuli, including PM and LPS, increase CXCR2 expression and CXCL-2 secretion in the lungs [116–119,123–125]. CXCL-2-induced migration is regulated by its-mediated Ca^{2+} signaling via the redox-regulated Ca^{2+}-permeable channel TRPC6, broadly expressed in the lungs and implicated in various pulmonary disorders including cystic fibrosis, asthma, pulmonary hypertension, and COPD [126]. PM-induced H_2O_2 in the lungs increases TRPC6 expression and activation, and enhances its sensitivity to diacylglycerol (DAG) [127]. Activation of CXCR2 by its ligand induces DAG generation, which in turn activates TRPC6, promoting intracellular Ca^{2+} influx and neutrophil recruitment into the lungs [128,129]. Consistent with our previous study that identified TRPC6 as a novel diagnostic biomarker of PM-induced COPD and observed increased *TRPC6* mRNA expression in PM-exposed RAW 264.7 cells [130], we observed increased TRPC6 expression in alveolar epithelial cells exposed to PM and LPS. Our results showed that GCN inhibited the expression of TNF-α, TRPC6, and CXCL-2 and reduced the phosphorylation of MAPK, NF-κB, and c-Jun in PM- and LPS-exposed lung epithelial cells, indicating suppression of MAPK–NF-κB/AP-1 signaling. Several GCN constituents could plausibly contribute to this effect. For example, β-glucan has been reported to attenuate LPS-driven inflammation by downregulating TLR4/MyD88 and suppressing ERK/JNK phosphorylation and NF-κB activation, thereby reducing pro-inflammatory mediator production [131–134]. Anthocyanins and related polyphenols can inhibit ROS generation and MAPK activation and enhance antioxidant defense, potentially reducing inflammatory outputs such as TNF-α [135,136]. Cordycepin has been reported to suppress NF-κB activation by inhibiting IκB-α degradation and NF-κB nuclear translocation and to modulate ERK/JNK phosphorylation and LPS–TLR4 interactions [137,138]. Similarly, isoflavones such as genistein and daidzein may interfere with LPS-induced TLR4/MyD88 signaling and attenuate NF-κB activation, thereby reducing cytokine and chemokine production [137,139,140]. Taken together, these results indicate that GCN reduces ROS accumulation and regulates MAPK–NF-κB/AP-1 signaling, thereby attenuating inflammatory responses in PM- and LPS-stimulated airway epithelial cells.

5. Conclusions

Overall, this study demonstrates that nano-encapsulation of GRC extract in CHI nanoparticles enhances its stability and bioactivity and provides mechanistic evidence for its protective effects against PM- and LPS-induced oxidative stress and inflammation. In A549 cells, GCN pretreatment attenuated inflammatory signaling by regulating TLR4-mediated MAPK–NF-κB/AP-1 pathways and suppressing key hub genes, including TNF-α and CXCL-2. These findings support the potential of nano-encapsulated GCN as a functional food-derived ingredient for mitigating environmentally induced pulmonary inflammatory responses and suggest relevant molecular targets as potential biomarkers.

Author Contributions: Conceptualization, H-J P.; methodology, H-J P., and H-M K.; validation H-J P., and H-M K.; investigation, H-J P., and H-M K.; Formal analysis, H-M K.; data curation, H-J P., and H-M K.; writing—original draft preparation, H-J P., and H-M K.; writing—review and editing, H-J P., and H-M K.; visualization, H-M K.; supervision, H-J P.; project administration, H-J P.; funding acquisition, H-J P. All authors have read and agreed to the published version of the manuscript.

Funding: This research received no external funding.

Institutional Review Board Statement: Not applicable.

Informed Consent Statement: Not applicable.

Data Availability Statement: Dataset available on request from the authors.

Acknowledgments: The authors thank Dong Ki Park and researchers from the Cell Activation Research Institute (CARI, Seoul, Korea) for sample preparation and technical support. The authors also thank Jong-Heon Kim for his assistance with Western blot and DCF-DA assays, as well as with some of the experiments.

 doi:10.20944/preprints202604.1362.v1

Conflicts of Interest: The authors declare no conflicts of interest.

References

1. Zomuansangi, R., et al., *Interaction of bacteria and inhalable particulate matter in respiratory infectious diseases caused by bacteria.* Atmospheric Pollution Research, 2024. **15**(3): p. 102012.
2. Gualtieri, M., et al., *Winter fine particulate matter from Milan induces morphological and functional alterations in human pulmonary epithelial cells (A549).* Toxicology letters, 2009. **188**(1): p. 52–62.
3. Dai, P., et al., *The roles of Nrf2 and autophagy in modulating inflammation mediated by TLR4-NFκB in A549 cell exposed to layer house particulate matter 2.5 (PM2. 5).* Chemosphere, 2019. **235**: p. 1134–1145.
4. Wang, Q. and S. Liu, *The effects and pathogenesis of PM2. 5 and its components on chronic obstructive pulmonary disease.* International journal of chronic obstructive pulmonary disease, 2023: p. 493–506.
5. Finnerty, K., et al., *Instillation of coarse ash particulate matter and lipopolysaccharide produces a systemic inflammatory response in mice.* Journal of Toxicology and Environmental Health, Part A, 2007. **70**(23): p. 1957–1966.
6. Sang, S., et al., *The global burden of disease attributable to ambient fine particulate matter in 204 countries and territories, 1990–2019: A systematic analysis of the Global Burden of Disease Study 2019.* Ecotoxicology and environmental safety, 2022. **238**: p. 113588.
7. Zhang, T., et al., *Protective effects of natural products against lung damage caused by fine particulate matter.* Environmental Pollution, 2025: p. 126942.
8. Wang, X., et al., *Mechanism of PM2. 5 induced/aggravated allergic diseases and its prevention and treatment.* Allergy Medicine, 2024. **2**: p. 100012.
9. Yue, G.G.-L., et al., *Effects of Cordyceps sinensis, Cordyceps militaris and their isolated compounds on ion transport in Calu-3 human airway epithelial cells.* Journal of Ethnopharmacology, 2008. **117**(1): p. 92–101.
10. Wang, X., et al., *Cordyceps militaris solid medium extract alleviates lipopolysaccharide-induced acute lung injury via regulating gut microbiota and metabolism.* Frontiers in Immunology, 2025. **15**: p. 1528222.
11. Chou, Y.-C., et al., *Current progress regarding Cordyceps militaris, its metabolite function, and its production.* Applied Sciences, 2024. **14**(11): p. 4610.
12. Das, S.K., et al., *Medicinal uses of the mushroom Cordyceps militaris: current state and prospects.* Fitoterapia, 2010. **81**(8): p. 961–968.
13. Phull, A.-R., M. Ahmed, and H.-J. Park, *Cordyceps militaris as a bio functional food source: pharmacological potential, anti-inflammatory actions and related molecular mechanisms.* Microorganisms, 2022. **10**(2): p. 405.
14. Zhang, J., et al., *Advance in Cordyceps militaris (Linn) Link polysaccharides: Isolation, structure, and bioactivities: A review.* International journal of biological macromolecules, 2019. **132**: p. 906–914.
15. Park, H.-J., *Influence of Culture Conditions on Bioactive Compounds in Cordyceps militaris: A Comprehensive Review.* Foods, 2025. **14**(19): p. 3408.
16. Phoungthong, K., et al., *Utilization of corncob biochar in cultivation media for Cordycepin production and biomass of Cordyceps militaris.* Sustainability, 2022. **14**(15): p. 9362.
17. Park, M.H. and M. Kim, *Antioxidant and anti-inflammatory activity and cytotoxicity of ethanol extracts from Rhynchosia nulubilis cultivated with Ganoderma lucidum mycelium.* Preventive nutrition and food science, 2018. **23**(4): p. 326.
18. Yu, S., H. Park, and W. Kim, *Anti-inflammaging effects of black soybean and black rice mixture extract by reprogramming of mitochondrial respirations in murine macrophages.* Journal of Functional Foods, 2022. **94**: p. 105114.
19. Wu, T., et al., *Exploring the effect of boiling processing on the metabolic components of black beans through* in vitro *simulated digestion.* LWT, 2023. **184**: p. 114987.
20. Kwon, H.-K., W.-R. Jo, and H.-J. Park, *Immune-enhancing activity of C. militaris fermented with Pediococcus pentosaceus (GRC-ON89A) in CY-induced immunosuppressed model.* BMC complementary and alternative medicine, 2018. **18**(1): p. 75.
21. Phull, A.-R., K.-R. Dhong, and H.-J. Park, *Lactic acid bacteria fermented Cordyceps militaris (GRC-SC11) suppresses ige mediated mast cell activation and type i hypersensitive allergic murine model.* Nutrients, 2021. **13**(11): p. 3849.

 doi:10.20944/preprints202604.1362.v1

22. Park, D.K. and H.-J. Park, *Ethanol Extract of Cordyceps militaris Grown on Germinated Soybeans Attenuates Dextran-Sodium-Sulfate-(DSS-) Induced Colitis by Suppressing the Expression of Matrix Metalloproteinases and Inflammatory Mediators.* BioMed Research International, 2013. **2013**(1): p. 102918.
23. Lee, H.-J. and H.-J. Park, *Germinated Rhynchosia nulubilis Fermented with Lactobacillus pentosus SC65 Reduces Particulate Matter Induced Type II Alveolar Epithelial Apoptotic Cell Death.* International Journal of Molecular Sciences, 2021. **22**(7): p. 3660.
24. Zhang, D.-N., et al., *An efficient enzymatic modification of cordycepin in ionic liquids under ultrasonic irradiation.* Ultrasonics sonochemistry, 2014. **21**(5): p. 1682–1687.
25. Gao, F., et al., *Unveiling the multifaceted roles of anthocyanins: a review of their bioavailability, impacts on gut and system health, and industrial implications.* Current Research in Food Science, 2025: p. 101137.
26. Alvarez-Suarez, J.M., et al., *Novel approaches in anthocyanin research-Plant fortification and bioavailability issues.* Trends in Food Science & Technology, 2021. **117**: p. 92–105.
27. Singla, A., et al., *Beta-glucan as a soluble dietary fiber source: Origins, biosynthesis, extraction, purification, structural characteristics, bioavailability, biofunctional attributes, industrial utilization, and global trade.* Nutrients, 2024. **16**(6): p. 900.
28. Xiao, Y., et al., *Synthesis, characterization, and evaluation of genistein-loaded zein/carboxymethyl chitosan nanoparticles with improved water dispersibility, enhanced antioxidant activity, and controlled release property.* Foods, 2020. **9**(11): p. 1604.
29. Scheepens, A., K. Tan, and J.W. Paxton, *Improving the oral bioavailability of beneficial polyphenols through designed synergies.* Genes & nutrition, 2010. **5**(1): p. 75–87.
30. Wu, Y., et al., *Chitosan nanoparticles efficiently enhance the dispersibility, stability and selective antibacterial activity of insoluble isoflavonoids.* International Journal of Biological Macromolecules, 2023. **232**: p. 123420.
31. Zhang, W., et al., *Microencapsulation of anthocyanins extracted from black soybean peels by whey protein/fructo-oligosaccharide contributes to improved stability, bioavailability, and ability to regulate glycolipid metabolism.* Food Frontiers, 2024. **5**(2): p. 570–583.
32. Marsup, P., et al., *Enhancement of chemical stability and dermal delivery of Cordyceps militaris extracts by nanoemulsion.* Nanomaterials, 2020. **10**(8): p. 1565.
33. Guadarrama-Escobar, O.R., et al., *Chitosan nanoparticles as oral drug carriers.* International journal of molecular sciences, 2023. **24**(5): p. 4289.
34. Cheng, X., et al., *Effects of a chitosan nanoparticles encapsulation on the properties of litchi polyphenols.* Food Science and Biotechnology, 2023. **32**(13): p. 1861–1871.
35. Park, B.-J., K.-R. Dhong, and H.-J. Park, *Cordyceps militaris Grown on Germinated Rhynchosia nulubilis (GRC) Encapsulated in Chitosan Nanoparticle (GCN) Suppresses Particulate Matter (PM)-Induced Lung Inflammation in Mice.* International Journal of Molecular Sciences, 2024. **25**(19): p. 10642.
36. Kim, H.-M., et al., *Chitosan Nanoparticle-Encapsulated Cordyceps militaris Grown on Germinated Rhynchosia nulubilis Reduces Type II Alveolar Epithelial Cell Apoptosis in PM2. 5-Induced Lung Injury.* International Journal of Molecular Sciences, 2025. **26**(3): p. 1105.
37. Wang, M., et al., *Preparing, optimising, and evaluating chitosan nanocapsules to improve the stability of anthocyanins from Aronia melanocarpa.* RSC advances, 2021. **11**(1): p. 210–218.
38. Zheng, S., et al., *Application of network pharmacology in traditional Chinese medicine for the treatment of digestive system diseases.* Frontiers in Pharmacology, 2024. **15**: p. 1412997.
39. Zhang, G.-b., et al., *Network pharmacology: a new approach for Chinese herbal medicine research.* Evidence-Based Complementary and Alternative Medicine, 2013. **2013**(1): p. 621423.
40. Lee, H.-J., H.-E. Cho, and H.-J. Park, *Germinated black soybean fermented with Lactobacillus pentosus SC65 alleviates DNFB-induced delayed-type hypersensitivity in C57BL/6N mice.* Journal of Ethnopharmacology, 2021. **265**: p. 113236.
41. Kim, H.-M., et al., *Chitosan Nanoparticle-Encapsulated Cordyceps militaris Grown on Germinated Rhynchosia nulubilis Reduces Type II Alveolar Epithelial Cell Apoptosis in PM2.5-Induced Lung Injury.* International Journal of Molecular Sciences, 2025. **26**(3): p. 1105.
42. Zeng, Y., et al., *Screening of hub genes associated with pulmonary arterial hypertension by integrated bioinformatic analysis.* BioMed research international, 2021. **2021**(1): p. 6626094.

 doi:10.20944/preprints202604.1362.v1

43. Yin, Y., et al., *Mechanism of YuPingFeng in the treatment of COPD based on network pharmacology.* BioMed Research International, 2020. **2020**(1): p. 1630102.
44. Harel, A., et al., *GIFtS: annotation landscape analysis with GeneCards.* BMC bioinformatics, 2009. **10**: p. 1–11.
45. Aziz, F., N. Shoaib, and A. Rehman, *Hub genes identification and association of key pathways with hypoxia in cancer cells: A bioinformatics analysis.* Saudi Journal of Biological Sciences, 2023. **30**(9): p. 103752.
46. Kumar, S., J.-J. Wee, and K.S. Kumar, *Identification of Common Hub Genes in COVID-19 and Comorbidities: Insights into Shared Molecular Pathways and Disease Severity.* COVID, 2025. **5**(7): p. 105.
47. Chin, C.-H., et al., *cytoHubba: identifying hub objects and sub-networks from complex interactome.* BMC systems biology, 2014. **8**: p. 1–7.
48. Dhong, K.-R., H.-K. Kwon, and H.-J. Park, *Immunostimulatory Activity of Cordyceps militaris Fermented with Pediococcus pentosaceus SC11 Isolated from a Salted Small Octopus in Cyclophosphamide-Induced Immunocompromised Mice and Its Inhibitory Activity against SARS-CoV 3CL Protease.* Microorganisms, 2022. **10**(12): p. 2321.
49. Kwon, H.-K. and H.-J. Park, *Phellinus linteus Grown on Germinated Brown Rice Inhibits IgE-Mediated Allergic Activity through the Suppression of FcεRI-Dependent Signaling Pathway* In Vitro *and* In Vivo. Evidence-Based Complementary and Alternative Medicine, 2019. **2019**.
50. Kwon, H.-K. and H.-J. Park, *Phellinus linteus Grown on Germinated Brown Rice Inhibits IgE-Mediated Allergic Activity through the Suppression of FcεRI-Dependent Signaling Pathway* In Vitro *and* In Vivo. Evidence-Based Complementary and Alternative Medicine, 2019. **2019**(1): p. 1485015.
51. Loffredo, C., et al., *PM2. 5 as a marker of exposure to tobacco smoke and other sources of particulate matter in Cairo, Egypt.* The International Journal of Tuberculosis and Lung Disease, 2016. **20**(3): p. 417–422.
52. Fehrenbach, H., *Alveolar epithelial type II cell: defender of the alveolus revisited.* Respiratory Research, 2001. **2**(1): p. 33.
53. Yang, J., et al., *The impact of bacteria-derived ultrafine dust particles on pulmonary diseases.* Experimental & molecular medicine, 2020. **52**(3): p. 338–347.
54. Mushtaq, N., et al., *Adhesion of Streptococcus pneumoniae to human airway epithelial cells exposed to urban particulate matter.* Journal of allergy and clinical immunology, 2011. **127**(5): p. 1236–1242. e2.
55. Kim, D.I., M.-K. Song, and K. Lee, *Diesel exhaust particulates enhances susceptibility of LPS-induced acute lung injury through upregulation of the IL-17 cytokine-derived TGF-β1/collagen i expression and activation of NLRP3 inflammasome signaling in mice.* Biomolecules, 2021. **11**(1): p. 67.
56. Kwon, H.-K., W.-R. Jo, and H.-J. Park, *Immune-enhancing activity of C. militaris fermented with Pediococcus pentosaceus (GRC-ON89A) in CY-induced immunosuppressed model.* BMC complementary and alternative medicine, 2018. **18**: p. 1–14.
57. Choi, J.N., et al., *Metabolomics revealed novel isoflavones and optimal cultivation time of Cordyceps militaris fermentation.* Journal of Agricultural and Food Chemistry, 2010. **58**(7): p. 4258–4267.
58. Park, H.-J., *The Genus Cordyceps Sensu Lato: Their Chemical Constituents, Biological Activities, and Therapeutic Effects on Air Pollutants Related to Lung and Vascular Diseases.* Life, 2025. **15**(6): p. 935.
59. Zhang, D.-N., et al., *An efficient enzymatic modification of cordycepin in ionic liquids under ultrasonic irradiation.* Ultrasonics sonochemistry, 2014. **21**(5): p. 1682–1687.
60. Scheepens, A., K. Tan, and J.W. Paxton, *Improving the oral bioavailability of beneficial polyphenols through designed synergies.* Genes & nutrition, 2010. **5**(1): p. 75–87.
61. Chen, M., et al., *Cordycepin: A review of strategies to improve the bioavailability and efficacy.* Phytotherapy Research, 2023. **37**(9): p. 3839–3858.
62. Dyawanapelly, S., et al., *Improved mucoadhesion and cell uptake of chitosan and chitosan oligosaccharide surface-modified polymer nanoparticles for mucosal delivery of proteins.* Drug Delivery and Translational Research, 2016. **6**(4): p. 365–379.
63. Kwon, H.-K., et al., *Pediococcus pentosaceus-fermented Cordyceps militaris inhibits inflammatory reactions and alleviates contact dermatitis.* International Journal of Molecular Sciences, 2018. **19**(11): p. 3504.
64. Yan, Z., et al., *The cytotoxic effects of fine particulate matter (PM2. 5) from different sources at the air–liquid interface exposure on a549 cells.* Toxics, 2023. **12**(1): p. 21.

 doi:10.20944/preprints202604.1362.v1

65. Harrison, R.M., *Airborne particulate matter.* Philosophical Transactions of the Royal Society A, 2020. **378**(2183): p. 20190319.
66. Wang, J., et al., *Urban particulate matter triggers lung inflammation via the ROS-MAPK-NF-κB signaling pathway.* Journal of thoracic disease, 2017. **9**(11): p. 4398.
67. Arlt, V.M., et al., *Pulmonary inflammation impacts on CYP1A1-mediated respiratory tract DNA damage induced by the carcinogenic air pollutant benzo [a] pyrene.* Toxicological Sciences, 2015. **146**(2): p. 213–225.
68. Androutsopoulos, V.P., A.M. Tsatsakis, and D.A. Spandidos, *Cytochrome P450 CYP1A1: wider roles in cancer progression and prevention.* BMC cancer, 2009. **9**: p. 1–17.
69. Longhin, E., et al., *Cell cycle alterations induced by urban PM2. 5 in bronchial epithelial cells: characterization of the process and possible mechanisms involved.* Particle and fibre toxicology, 2013. **10**: p. 1–19.
70. Valavanidis, A., et al., *Electron paramagnetic resonance study of the generation of reactive oxygen species catalysed by transition metals and quinoid redox cycling by inhalable ambient particulate matter.* Redox Report, 2005. **10**(1): p. 37–51.
71. Pardo, M., et al., *Particulate matter toxicity is Nrf2 and mitochondria dependent: the roles of metals and polycyclic aromatic hydrocarbons.* Chemical research in toxicology, 2020. **33**(5): p. 1110–1120.
72. Valgimigli, L., et al., *The unusual reaction of semiquinone radicals with molecular oxygen.* The Journal of organic chemistry, 2008. **73**(5): p. 1830–1841.
73. Park, S., et al., *Potential toxicity of inorganic ions in particulate matter: Ion permeation in lung and disruption of cell metabolism.* Science of The Total Environment, 2022. **824**: p. 153818.
74. Scheres Firak, D., et al., *Ionic Strength Effect in Fenton Reactions in the Presence of Sulfate and Its Influence on the Aqueous Particle Phase.* ACS Earth and Space Chemistry, 2025. **9**(3): p. 662–670.
75. Li, H., et al., *Insight into urban PM2. 5 chemical composition and environmentally persistent free radicals attributed human lung epithelial cytotoxicity.* Ecotoxicology and Environmental Safety, 2022. **234**: p. 113356.
76. Di, A., et al., *Chemical characterization of seasonal PM2. 5 samples and their cytotoxicity in human lung epithelial cells (A549).* International Journal of Environmental Research and Public Health, 2020. **17**(12): p. 4599.
77. Xing, Y.-F., et al., *The impact of PM2. 5 on the human respiratory system.* Journal of thoracic disease, 2016. **8**(1): p. E69.
78. Wei, J., T. Fang, and M. Shiraiwa, *Effects of acidity on reactive oxygen species formation from secondary organic aerosols.* ACS environmental Au, 2022. **2**(4): p. 336–345.
79. Shahpoury, P., et al., *Influence of aerosol acidity and organic ligands on transition metal solubility and oxidative potential of fine particulate matter in urban environments.* Science of the Total Environment, 2024. **906**: p. 167405.
80. Fang, T., et al., *Oxidative potential of particulate matter and generation of reactive oxygen species in epithelial lining fluid.* Environmental science & technology, 2019. **53**(21): p. 12784–12792.
81. He, M., et al., *Role of iron and oxidative stress in the exacerbation of allergic inflammation in murine lungs caused by urban particulate matter< 2.5 μm and desert dust.* Journal of Applied Toxicology, 2019. **39**(6): p. 855–867.
82. Birben, E., et al., *Oxidative stress and antioxidant defense.* World allergy organization journal, 2012. **5**(1): p. 9–19.
83. Wang, Y., et al., *Poldip2/Nox4 Mediates Lipopolysaccharide-Induced Oxidative Stress and Inflammation in Human Lung Epithelial Cells.* Mediators of Inflammation, 2022. **2022**(1): p. 6666022.
84. Sul, O.-J. and S.W. Ra, *Quercetin Prevents LPS-Induced Oxidative Stress and Inflammation by Modulating NOX2/ROS/NF-kB in Lung Epithelial Cells.* Molecules, 2021. **26**(22): p. 6949.
85. Mandaglio-Collados, D., et al., *Analysis of Key Proinflammatory Mechanisms in Cardiovascular Pathology through Stimulation with Lipopolysaccharide and Urban Particulate Matter in Mouse Atrial Cardiomyocytes.* Environmental Toxicology and Pharmacology, 2025: p. 104652.
86. Chen, W., et al., *Effects of real-ambient PM2. 5 exposure plus lipopolysaccharide on multiple organ damage in mice.* Human & Experimental Toxicology, 2022. **41**: p. 09603271211061505.
87. Chen, X., et al., *Urban particulate matter (PM) suppresses airway antibacterial defence.* Respiratory research, 2018. **19**: p. 1–11.
88. Gamboa, J.M. and K.W. Leong, In vitro *and* in vivo *models for the study of oral delivery of nanoparticles.* Advanced drug delivery reviews, 2013. **65**(6): p. 800–810.

 doi:10.20944/preprints202604.1362.v1

89. Olatunji, O.J., et al., *Neuroprotective effects of adenosine isolated from Cordyceps cicadae against oxidative and ER stress damages induced by glutamate in PC12 cells.* Environmental toxicology and pharmacology, 2016. **44**: p. 53–61.
90. Wang, Z., et al., *Cordycepin prevents radiation ulcer by inhibiting cell senescence via NRF2 and AMPK in rodents.* Nature communications, 2019. **10**(1): p. 2538.
91. Won, K.-J., et al., *Cordycepin attenuates neointimal formation by inhibiting reactive oxygen species–mediated responses in vascular smooth muscle cells in rats.* Journal of pharmacological sciences, 2009. **109**(3): p. 403–412.
92. Yamashita, Y., et al., *Insights into the potential benefits of black soybean (Glycine max L.) polyphenols in lifestyle diseases.* Food & Function, 2020. **11**(9): p. 7321–7339.
93. Yu, H.M., et al., *Comparison of protective effects between cultured Cordyceps militaris and natural Cordyceps sinensis against oxidative damage.* Journal of Agricultural and Food Chemistry, 2006. **54**(8): p. 3132–3138.
94. Nguyen, T.Q., et al., *Cordyceps militaris-Derived Bioactive Gels: Therapeutic and Anti-Aging Applications in Dermatology.* Gels, 2025. **11**(1): p. 33.
95. Yu, R., et al., *Structural elucidation and biological activity of a novel polysaccharide by alkaline extraction from cultured Cordyceps militaris.* Carbohydrate polymers, 2009. **75**(1): p. 166–171.
96. Khan, A.A., et al., *Structural, rheological, antioxidant, and functional properties of β–glucan extracted from edible mushrooms Agaricus bisporus, Pleurotus ostreatus and Coprinus attrimentarius.* Bioactive Carbohydrates and Dietary Fibre, 2017. **11**: p. 67–74.
97. Arunachalam, K., P.S. Sreeja, and X. Yang, *The antioxidant properties of mushroom polysaccharides can potentially mitigate oxidative stress, beta-cell dysfunction and insulin resistance.* Frontiers in Pharmacology, 2022. **13**: p. 874474.
98. Ru, Q., et al., *Lipopolysaccharide accelerates fine particulate matter-induced cell apoptosis in human lung bronchial epithelial cells.* International Journal of Occupational Medicine and Environmental Health, 2017. **31**(2): p. 173–183.
99. Wu, Y., et al., *Air pollutants and lung regeneration: impact on the fate of lung stem cells.* Environment International, 2025. **199**: p. 109525.
100. Liu, Q., et al., *Attenuation of PM(2.5)-induced alveolar epithelial cells and lung injury through regulation of mitochondrial fission and fusion.* Part Fibre Toxicol, 2023. **20**(1): p. 28.
101. Wang, F., et al., *LPS-induced inflammatory response and apoptosis are mediated by Fra-1 upregulation and binding to YKL-40 in A549 cells.* Exp Ther Med, 2021. **22**(6): p. 1474.
102. Shu, J., et al., *Comparison and evaluation of two different methods to establish the cigarette smoke exposure mouse model of COPD.* Scientific Reports, 2017. **7**(1): p. 15454.
103. Kim, D.I., M.K. Song, and K. Lee, *Diesel Exhaust Particulates Enhances Susceptibility of LPS-Induced Acute Lung Injury through Upregulation of the IL-17 Cytokine-Derived TGF-β(1)/Collagen I Expression and Activation of NLRP3 Inflammasome Signaling in Mice.* Biomolecules, 2021. **11**(1).
104. Fonceca, A.M., et al., *Accumulation mode particles and LPS exposure induce TLR-4 dependent and independent inflammatory responses in the lung.* Respiratory Research, 2018. **19**(1): p. 15.
105. Shim, S. and H.S. Yoo, *The Application of Mucoadhesive Chitosan Nanoparticles in Nasal Drug Delivery.* Mar Drugs, 2020. **18**(12).
106. Lee, H.J., et al., *Hair Growth Promoting Effect of 4HGF Encapsulated with PGA Nanoparticles (PGA-4HGF) by β-Catenin Activation and Its Related Cell Cycle Molecules.* Int J Mol Sci, 2019. **20**(14).
107. Fetterman, J.L., M.J. Sammy, and S.W. Ballinger, *Mitochondrial toxicity of tobacco smoke and air pollution.* Toxicology, 2017. **391**: p. 18–33.
108. Pappas, R.S., *Toxic elements in tobacco and in cigarette smoke: inflammation and sensitization.* Metallomics, 2011. **3**(11): p. 1181–1198.
109. Wang, Q. and S. Liu, *The effects and pathogenesis of PM2. 5 and its components on chronic obstructive pulmonary disease.* International Journal of Chronic Obstructive Pulmonary Disease, 2023: p. 493–506.
110. Korsgren, M., et al., *Inhalation of LPS induces inflammatory airway responses mimicking characteristics of chronic obstructive pulmonary disease.* Clinical physiology and functional imaging, 2012. **32**(1): p. 71–79.

 doi:10.20944/preprints202604.1362.v1

111. Feng, Q., Y.-Z. Yu, and Q.-H. Meng, *Blocking tumor necrosis factor-α delays progression of chronic obstructive pulmonary disease in rats through inhibiting MAPK signaling pathway and activating SOCS3/TRAF1.* Experimental and therapeutic medicine, 2021. **22**(5): p. 1311.
112. Ahmadi, A., et al., *p38 MAPK signaling in chronic obstructive pulmonary disease pathogenesis and inhibitor therapeutics.* Cell Communication and Signaling, 2023. **21**(1): p. 314.
113. Schuliga, M., *NF-kappaB signaling in chronic inflammatory airway disease.* Biomolecules, 2015. **5**(3): p. 1266–1283.
114. Sidletskaya, K., T. Vitkina, and Y. Denisenko, *The role of toll-like receptors 2 and 4 in the pathogenesis of chronic obstructive pulmonary disease.* International journal of chronic obstructive pulmonary disease, 2020: p. 1481–1493.
115. Zhang, Q., et al., *scRNA-seq and scATAC-seq analyses highlight the role of TNF signaling pathway in chronic obstructive pulmonary disease model mice.* PloS one, 2025. **20**(5): p. e0322538.
116. Yi, G., et al., *A large lung gene expression study identifying IL1B as a novel player in airway inflammation in COPD airway epithelial cells.* Inflammation Research, 2018. **67**: p. 539–551.
117. Jing, H., et al., *Inhibition of CXC motif chemokine 10 (CXCL10) protects mice from cigarette smoke-induced chronic obstructive pulmonary disease.* Medical Science Monitor: International Medical Journal of Experimental and Clinical Research, 2018. **24**: p. 5748.
118. Lappalainen, U., et al., *Interleukin-1β causes pulmonary inflammation, emphysema, and airway remodeling in the adult murine lung.* American journal of respiratory cell and molecular biology, 2005. **32**(4): p. 311–318.
119. Liu, C.-W., et al., *PM 2.5-induced oxidative stress increases intercellular adhesion molecule-1 expression in lung epithelial cells through the IL-6/AKT/STAT3/NF-κB-dependent pathway.* Particle and fibre toxicology, 2018. **15**: p. 1–16.
120. He, M., et al., *PM2. 5-induced lung inflammation in mice: Differences of inflammatory response in macrophages and type II alveolar cells.* Journal of Applied Toxicology, 2017. **37**(10): p. 1203–1218.
121. Wu, Y.-F., et al., *Inactivation of MTOR promotes autophagy-mediated epithelial injury in particulate matter-induced airway inflammation.* Autophagy, 2020. **16**(3): p. 435–450.
122. Yanagisawa, R., et al., *Gene expression analysis of murine lungs following pulmonary exposure to Asian sand dust particles.* Experimental Biology and Medicine, 2007. **232**(8): p. 1109–1118.
123. Russo, R.C. and B. Ryffel, *The chemokine system as a key regulator of pulmonary fibrosis: Converging pathways in human idiopathic pulmonary fibrosis (IPF) and the bleomycin-induced lung fibrosis model in mice.* Cells, 2024. **13**(24): p. 2058.
124. Li, Y.-J., et al., *Nrf2 lowers the risk of lung injury via modulating the airway innate immune response induced by diesel exhaust in mice.* Biomedicines, 2020. **8**(10): p. 443.
125. Liu, J., et al., *Increased alveolar epithelial TRAF6 via autophagy-dependent TRIM37 degradation mediates particulate matter-induced lung metastasis.* Autophagy, 2022. **18**(5): p. 971–989.
126. Chen, Q., et al., *TRPC6-dependent Ca2+ signaling mediates airway inflammation in response to oxidative stress via ERK pathway.* Cell Death & Disease, 2020. **11**(3): p. 170.
127. Chen, Q.-Z., et al., *TRPC6 modulates adhesion of neutrophils to airway epithelial cells via NF-κB activation and ICAM-1 expression with ozone exposure.* Experimental cell research, 2019. **377**(1–2): p. 56–66.
128. Vlag, J. and T. Nijenhuis, *A Putative Role for TRPC6 in Immune-Mediated Kidney Injury.* 2023.
129. Lindemann, O., et al., *Intravascular adhesion and recruitment of neutrophils in response to CXCL1 depends on their TRPC6 channels.* Journal of Molecular Medicine, 2020. **98**(3): p. 349–360.
130. Dhong, K.-R., et al., *Identification of TRPC6 as a novel diagnostic biomarker of PM-induced chronic obstructive pulmonary disease using machine learning models.* Genes, 2023. **14**(2): p. 284.
131. Du, B., et al., *An insight into anti-inflammatory effects of fungal beta-glucans.* Trends in Food Science & Technology, 2015. **41**(1): p. 49–59.
132. Moniruzzaman, M., et al., *A review on pharmacological insights of edible and medicinal mushroom based β-glucans.* Applied Biological Chemistry, 2025. **68**(1): p. 41.
133. Zhu, W., et al., *β-Glucan modulates the lipopolysaccharide-induced innate immune response in rat mammary epithelial cells.* International immunopharmacology, 2013. **15**(2): p. 457–465.

 doi:10.20944/preprints202604.1362.v1

134. Smiderle, F.R., et al., *Anti-inflammatory properties of the medicinal mushroom Cordyceps militaris might be related to its linear (1→ 3)-β-D-glucan.* PLoS One, 2014. **9**(10): p. e110266.
135. Chen, X.-Y., et al., *Black rice anthocyanins suppress metastasis of breast cancer cells by targeting RAS/RAF/MAPK pathway.* BioMed research international, 2015. **2015**(1): p. 414250.
136. Kim, J.N., et al., *Black soybean anthocyanins attenuate inflammatory responses by suppressing reactive oxygen species production and mitogen activated protein kinases signaling in lipopolysaccharide-stimulated macrophages.* Nutrition Research and Practice, 2017. **11**(5): p. 357–364.
137. Choi, Y.H., G.-Y. Kim, and H.H. Lee, *Anti-inflammatory effects of cordycepin in lipopolysaccharide-stimulated RAW 264.7 macrophages through Toll-like receptor 4-mediated suppression of mitogen-activated protein kinases and NF-κB signaling pathways.* Drug design, development and therapy, 2014: p. 1941–1953.
138. Lei, J., et al., *Cordycepin inhibits LPS-induced acute lung injury by inhibiting inflammation and oxidative stress.* European Journal of Pharmacology, 2018. **818**: p. 110–114.
139. Feng, G., B. Sun, and T.-z. Li, *Daidzein attenuates lipopolysaccharide-induced acute lung injury via toll-like receptor 4/NF-kappaB pathway.* International immunopharmacology, 2015. **26**(2): p. 392–400.
140. Kojima, K., et al., *Isoflavone aglycones attenuate cigarette smoke-induced emphysema via suppression of neutrophilic inflammation in a COPD murine model.* Nutrients, 2019. **11**(9): p. 2023.